FEBS Letters 585 (2011) 71–77

FEBS Letters
journal homepage: www.FEBSLetters.org

Porcine islet amyloid polypeptide fragments are refractory to amyloid formation

Xin Zhang [a], Biao Cheng [a], Hao Gong [a], Chuanzhou Li [b], Hong Chen [a], Ling Zheng [b,*], Kun Huang [a,*]

[a] Tongji School of Pharmacy, Huazhong University of Science and Technology, Wuhan, Hubei 430030, PR China
[b] College of Life Sciences, Wuhan University, Wuhan, Hubei 430072, PR China

ARTICLE INFO

Article history:
Received 22 September 2010
Revised 17 November 2010
Accepted 25 November 2010
Available online 3 December 2010

Edited by Jesus Avila

Keywords:
Amylin
Amyloid fibril
IAPP
Oligomerization
Seeding
Type 2 diabetes mellitus

ABSTRACT

Of 10 variation sites between sequences of amyloid-resistant porcine islet amyloid polypeptide (pIAPP) and amyloid-prone human IAPP (hIAPP), seven locate within residues 17–29, the most amyloidogenic fragment within hIAPP. To investigate how these variations affect amyloidogenicity, 26 IAPP(17–29) or IAPP(20–29) variants were synthesized and their secondary structures, amyloidogenicity, oligomerization and cytotoxicity were studied. Our results indicated that pIAPP fragments are refractory to amyloid formation and significantly less cytotoxic compared with hIAPP fragments. A novel stable dimer was observed in pIAPP(20–29) solution, whereas hIAPP(20–29) exists mostly as monomers and trimers. Among all human to porcine substitutions, S20R caused the most prolonged lag time and significantly attenuated cytotoxicity. The different oligomerization and amyloidogenic properties of hIAPP and pIAPP fragments are discussed.

Structured summary:
pIAPP and pIAPP *bind*: shown by *molecular sieving* (view interactions 1, 2)
hIAPP and hIAPP *bind*: shown by *molecular sieving* (view interactions 1, 2)

1. Introduction

The formation of amyloid aggregates by human islet amyloid polypeptide (hIAPP, also known as amylin) is regarded as a major causative factor of type 2 diabetes (T2DM) [1]. IAPP is a 37-residue peptide hormone synthesized by the pancreatic β-cells [2]. It has been documented that both human and feline IAPP are prone to form toxic aggregates, whereas IAPP from rodents such as rat and degu are resistant to this process [3]. In an elegant recent study, Potter et al. reported that porcine IAPP (pIAPP) is significantly less amyloidogenic compared with hIAPP, thus supporting the potential application of porcine islet transplantation in T2DM therapy [4]. Sequence comparison shows 10 variation sites between hIAPP and pIAPP (bold in Fig. 1). Notably, seven out of these 10 sites are located within the region of residues 17–29, with five of these being found between residues 20 and 29. These have been suggested to be the most critical and aggregation-prone regions for hIAPP amyloid formation [3,5,6].

To investigate how these sequence variations affect the amyloidogenic properties of IAPP, we studied the effects of substituting these sites with residues from the corresponding human or porcine residues in the templates of IAPP(17–29) and IAPP(20–29), which have been widely used as model peptide fragments in studying the amyloid formation of IAPP [3,7]. A set of 26 IAPP peptide fragments were chemically synthesized and their secondary structures, oligomerization and amyloidogenicity were tested. Our results demonstrated that pIAPP(17–29) and pIAPP(20–29) fragments were refractory to form amyloid aggregates, whereas all hIAPP(20–29) or hIAPP(17–29) variants carrying single or multiple porcine substitutions showed certain degrees of prolonged fibrillation lag time, with an arginine substitution at position 20 resulting in the most prolonged lag time. Furthermore, we showed that pIAPP(20–29) forms a novel stable dimer, whereas hIAPP(20–29) exists as monomers and trimers, implicating a potential link between oligomerization and amyloidogenecity. Possible mechanisms on the role of oligomerization involvement in amyloid formation are then discussed from a structural perspective.

Abbreviations: CD, circular dichroism; HFIP, hexafluoroisopropanol; IAPP, islet amyloid polypeptide; MTT, 3-(4,5-Dimethylthiazol-2-yl)-2,5-diphenyltetrazolium bromide; SEC, size-exclusion chromatography; SPPS, solid phase peptide synthesis; T2DM, type 2 diabetes mellitus; TEM, transmission electron-microscopy; TFE, trifluoroethanol; ThT, thioflavin-T. All amino acid residues are designated by standard one- and three-letter codes

* Corresponding authors.
E-mail addresses: lzheng217@hotmail.com (L. Zheng), kunhuang2008@hotmail.com (K. Huang).

0014-5793/$36.00 © 2010 Federation of European Biochemical Societies. Published by Elsevier B.V. All rights reserved.
doi:10.1016/j.febslet.2010.11.050

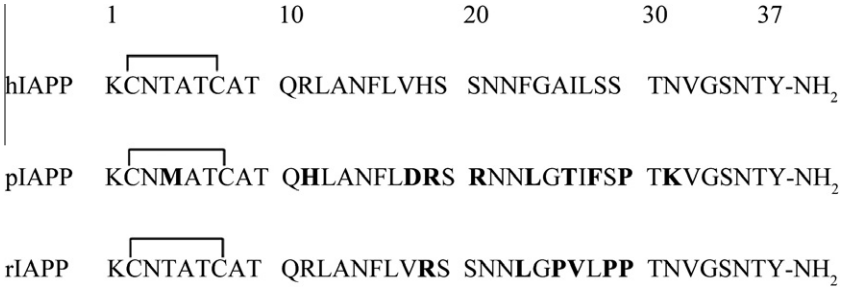

Fig. 1. Primary sequences of hIAPP, pIAPP and rIAPP. All peptides have an amidated C terminus and a disulfide bridge between Cys-2 and Cys-7. Residues differing from the human IAPP are indicated in bold.

2. Materials and methods

2.1. Materials

Synthetic hIAPP(1–37) was obtained from Genscript Inc. (Piscataway, NJ, USA). All reagents for peptide synthesis were obtained from GL Chemicals Ltd. (Shanghai, China). Hexafluoroisopropanol (HFIP) and thioflavin-T (ThT) were purchased from Sigma–Aldrich (St. Louis, USA). The INS-1 cells were obtained from the China Center for Type Culture Collection (CCTCC). All other chemicals were of the highest grade available.

2.2. Peptide synthesis and purification

All decapeptides (IAPP(20–29)) and tridecapeptides (IAPP(17–29)) were manually synthesized using standard 9-fluorenylmethyl chloroformate-based solid-phase peptide synthesis (SPPS) methodology as we previously described [8]. Crude peptides were purified by reverse phase high performance liquid chromatography using C4 semi-preparative or analytical column (Kromasil, AkzoNobel, Netherlands), and their identities were confirmed by ESI-MS.

2.3. Far-UV circular dichroism (CD) and data analysis

The CD spectra were recorded at 25 °C under a constant flow of N_2 by using a JASCO-810 spectropolarimeter (Tokyo, Japan). Data were recorded from 260 to 190 nm with a 1 mm pathlength. Purified peptide was dissolved in 50 mM sodium phosphate buffer (pH 7.4) containing 100 mM NaCl and 1% HFIP, or with 50% trifluoroethanol (TFE) co-solvent. The final peptide concentration was 10 μM (hIAPP(1–37)) or 100 μM (all other peptides). The spectra were recorded with a scanning speed of 20 nm/min, a response time of 1 s and a bandwidth of 2 nm. Each result was the average of three measurements. The data were converted to mean residue ellipticity [θ] and were further analyzed by the software package CDPro as we and others previously described [9,10]. Two reference data sets – SDP 42 (#6) and SDP 48 (#7) – were used in CDPro analysis since they both include denatured proteins [10].

2.4. Thioflavin-T (ThT) fluorescence assay and Aggrescan software analysis

Purified peptides were first dissolved in HFIP and sonicated for 2 min to homogenize the sample. The peptide solutions were further diluted to a final assay solution containing 50 mM sodium phosphate, 100 mM NaCl, 2% HFIP, 16.7 μM ThT and 100 μM peptide (except hIAPP, which was 20 μM), pH 7.4. The experiments were performed on a Hitachi FL-2700 fluorometer equipped with a kinetic measurement module and a thermostat water-pump system. The samples were incubated at 37 °C in a quartz cuvette with constant stirring at a fixed rate of 800 rpm. The excitation and emission wavelengths were set at 450 nm and 482 nm, respectively. The seeding experiments (self- or cross-seeding) were performed as we previously described [9,11]. Briefly, freshly prepared amyloids were sonicated for 3 min and immediately applied to fresh sample solution at 5% (w/w) final concentration as seeds. All experiments were repeated at least three times. The following formula was used to fit the kinetic curves as described [12,13], the t_{50} is described as time at half-maximum intensity, and the lag time is described as $t_{50} - 2/k$:

$$Y = Y_0 + (Y_{max} - Y_0)/[1 + \exp -(t - t_{50})k]$$

The amyloidogenic propensities of peptides were also predicted with the program Aggrescan as described [14].

2.5. Transmission electronic microscopy (TEM)

The TEM was performed as we previously described [11]. Briefly, 5-μl samples were applied to a 300-mesh Formvar-carbon coated copper grid (Shanghai, China), followed by staining with 1% fresh prepared uranyl formate, air dried and observed under a transmission microscope (Hitachi, Tokyo, Japan) operating at accelerating voltages of 100 kV.

2.6. Size-exclusion chromatograph (SEC)

The SEC analysis was performed on a Tosoh TSK GW2000 column (Tokyo, Japan) eluted with a 50 mM phosphate buffer containing 100 mM NaCl, pH 7.2 with a flow rate of 0.5 ml/min. Bovine serum albumin, ovalbumin, hen egg-white lysozyme, trypsin, RNAase A, porcine insulin, human glucagon-like peptide-1 amide (7–36) and an octapeptide (MW 854.9) were used for molecular weight calibration.

2.7. Cell toxicity assays

INS-1 cells were cultured in phenol red-free RPMI 1640 media containing 10% FBS, 1% sodium pyruvate and 50 μM β-mecaptoethanol. The 96-well plates were coated with 0.1% gelatin before use. The cells were plated at a density of 5×10^3 cells/well. Following 24-h incubation at 37 °C in 5% CO_2 atmosphere, fresh medium containing 100- or 200-μM different peptide fragments was added and further incubated for 24 h. Wells treated with medium containing the same amount of PBS were used as a negative control. After incubation, 20-μl 3-(4,5-dimethylthiazol-2-yl)-2,5-diphenyltetrazolium bromide (MTT) (5 mg/ml) was added to each well and incubated for 4 h. The absorbance was then measured at 570 nm. The average absorbance of the PBS-treated cells was set as 100% cell viability. Each treatment was repeated at least three times. All results were expressed as the mean ± S.D. Statistical significance was evaluated with the Kruskal–Wallis test [15], followed

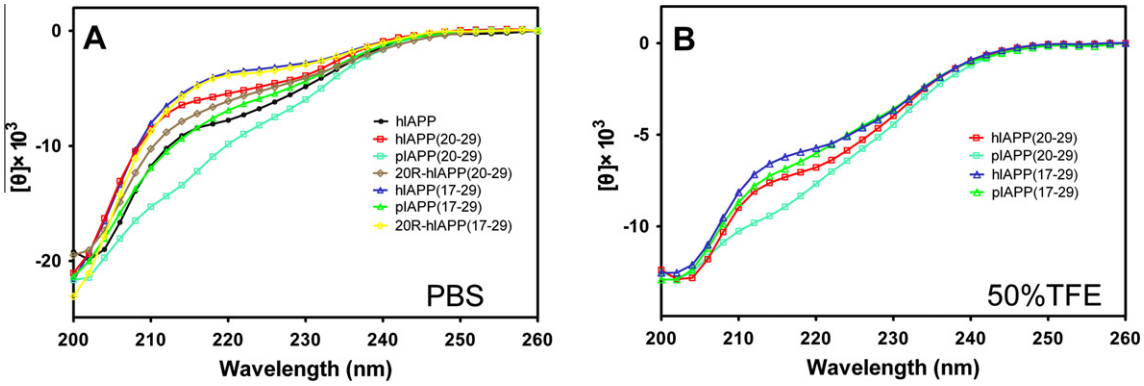

Fig. 2. Far-UV CD spectroscopy of IAPP fragments. Spectra were recorded at 25 °C in PBS buffer (A) or with 50% TFE (B).

by the Mann–Whitney test [15]. Differences were considered statistically significant at $P < 0.05$.

3. Results

3.1. Peptide synthesis

Twenty-six IAPP peptide fragments were manually synthesized and purified (for sequence details see Supplementary Fig. S1). Their identities were confirmed by ESI-MS (data not shown).

3.2. Secondary structures determination by far-UV CD and spectra deconvolution

To investigate the secondary structures of peptide fragment variants synthesized, far-UV CD spectroscopy was applied. Spectra were recorded in PBS buffer containing 1% HFIP.[1] Overall, CD spectra of hIAPP(1–37) and IAPP fragments were characteristic of predominant random coil structure (Fig. 2A and Supplementary Fig. S2), and supported by further CDPro deconvolution analysis[2] (Supplementary Fig. S3 and Table S1), which agreed with the previous reports [16,17]. It is of interest to note that spectra showed modest differences in the region of 210–230 nm between the hIAPP and pIAPP fragments, where spectra of hIAPP(20–29) and hIAPP(17–29) showed more positive CD signals than those of pIAPP(20–29) and pIAPP(17–29) (Fig. 2A).

CD spectra were also recorded in the presence of 50% TFE (Fig. 2B). Compared with spectra collected in PBS, further deconvolution analysis suggested a greatly increased extent of secondary structural components in 50% TFE (Supplementary Fig. S3 and Table S2). These differences found between the spectra in 50% TFE and PBS were, however, not as dramatic as previously reported [18]. Spectral differences between hIAPP and pIAPP fragments were still observed, however (Fig. 2B).

3.3. Amyloid formation

We first examined the amyloidogenic properties of IAPP(17–29) fragments. The ThT-binding assays suggested that under our experimental conditions, hIAPP(17–29) readily formed typical long linear amyloid fibrils (Fig. 3) and gave strong ThT emission with a short lag time of 39.1 ± 10.0 min (Table 1). In contrast, pIAPP(17–29) was rather refractory to amyloid formation under testing conditions, with more than 24 h constant stirring at 37 °C failing to raise ThT fluorescence. Only proteinaceous pIAPP(17–29) precipitates but not linear fibrils were observed under TEM (Fig. 3 and Table 1). pIAPP differs from hIAPP between residues 17 and 20 in three sites: 17D, 18R and 20R (Fig. 1). Among these sites, 17D and 20R exist only in porcine, whereas 18R is also present in species like rodent, chicken and feline. To test their impacts on the amyloidogenicity of IAPP, fourteen analogs were synthesized in IAPP(17–29) templates (human or porcine, Supplementary Fig. S1). Our results suggested that both 17D and 18R substitutions show minor impacts on the fibrillation of hIAPP(17–29). For hIAPP(17–29) carrying single 17D mutation or 17D18R double mutations, slightly lengthened lag times of 66.9 ± 12.9 min and 64.7 ± 17.5 min were observed as compared with the control hIAPP(17–29) (39.1 ± 10.0 min) (Table 1). In contrast, 20R-hIAPP(17–29) showed a dramatically prolonged lag time compared with hIAPP(17–29) (241.5 ± 114.0 min vs. 39.1 ± 10.0 min). Next, we tested the fibrillation properties of hIAPP(17–29) carrying 17D20R double substitutions or 17D18R20R triple substitutions, in which lengthened lag times of 329.2 ± 30.7 min and 283.8 ± 88.2 min were observed (Table 1), suggesting that 20R may play an important role in prolonging the lag time in pIAPP(217–229). We further applied pIAPP(17–29) as a template to test the impact of corresponding human substitutions (17V, 18H and 20S). Interestingly, none of these substitutions (single or combined) cause amyloid formation after stirring for up to 8 h at 37 °C (Table 1 and Supplementary Fig. S4).

We next synthesized nine IAPP(20–29) analogs and tested how five additional variant sites (Fig. 1) may affect the amyloidogenicity in the IAPP(20–29) template. ThT-fluorescence and TEM assays suggested that hIAPP(20–29) readily gave strong ThT fluorescence emission and formed long-linear amyloid fibrils with a short lag time of 39.6 ± 15.7 min (Fig. 3 and Table 1). Conversely, no positive ThT emission or fibrils were observed for pIAPP(20–29) even after agitation for more than 30 h (Fig. 3 and Table 1). Fibrillation of four hIAPP(20–29) analogs carrying single porcine substitution (20R, 23L, 25T and 27F) was also examined.[3] Our results suggested that the fibrillation lag times of analogs 20R-, 23L-, 25T- and 27F-hIAPP(20–29) fell in the order of 20R > 27F > 25T > 23L (Table 1), in which the 20R-hIAPP(20–29) analog showed a drastic 10-fold prolonged lag time (401.4 ± 116.4 min vs. 39.6 ± 15.7 min), which was in good accord with what we observed in the IAPP(17–29) samples. For position 20, amyloidogenecity of glycine and lysine substitutions was also examined. ThT assays showed that 20G-hIAPP(20–29)

[1] Control experiments showed that 1% HFIP in buffer does not interfere with the secondary structures of tested peptides (data not shown).

[2] Since CDPro utilizes mostly large globular proteins in its reference data sets, therefore analysis results for our short and highly flexible IAPP peptide fragments are subject to larger uncertainties than analysis of globular proteins.

[3] We were unable to synthesize enough 29P-hIAPP(20–29) analogue for assays, however, based on previous studies by Westermark et al. [3], 29P-hIAPP(20–29) shows similar amyloidogenic property as hIAPP(20–29), but is relatively slow in forming amyloids.

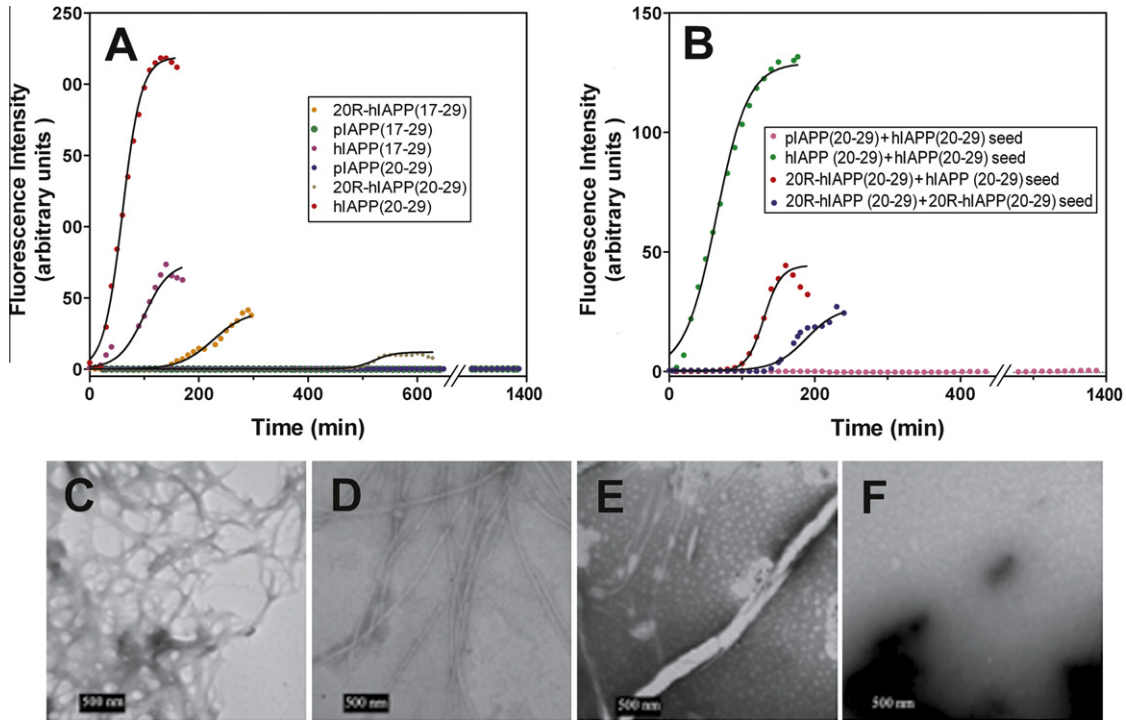

Fig. 3. Amyloidogenic properties of IAPP fragments as monitored with ThT fluorescence and TEM. (A) ThT-fluorescence of selected hIAPP fragments and pIAPP fragments; (B) seeding assays of hIAPP(20–29), 20R-hIAPP(20–29) and pIAPP(20–29); and (C)–(F) TEM images of hIAPP(1–37) (C), hIAPP(20–29) (D), 20R-hIAPP(20–29) (E) and pIAPP(20–29) (F).

aggregates even faster than the control hIAPP(20–29) (12.5 ± 3.6 min vs. 39.6 ± 15.7 min), whereas 20 K substitution results in a 7-fold increase in lag time (288.2 ± 24.4 min vs. 39.6 ± 15.7 min). However, no direct correlations were identified between experimentally measured lag times and the software Aggrescan predicted values (Table 1).

Next, seeding experiments were performed for samples hIAPP(20–29), pIAPP(20–29) and 20R-hIAPP(20–29). Results suggested that 5% freshly prepared hIAPP(20–29) seed significantly shortened the lag phase of itself (Table 1), which agreed with the previous report [19]. On the contrary, hIAPP(20–29) seed failed to induce pIAPP(20–29) amyloid formation even after co-incubation for 8 h (Fig. 3B). However, hIAPP(20–29) seed did promote the fibrillation of 20R-hIAPP(20–29) (lag time 181.5 ± 90.1 min vs. 401.4 ± 116.4 min, Fig. 3B). On the other hand, although 5% freshly prepared 20R-hIAPP(20–29) seed shortened the fibrillation lag time of itself (184.6 ± 32.2 min vs. 401.4 ± 116.4 min, Fig. 3B), it failed to promote the fibrillation of hIAPP(20–29) (lag time 65.6 ± 3.9 min vs. 39.6 ± 15.7 min).

3.4. Peptide oligomerization studied by SEC

To investigate the oligomerization of IAPP fragments, SEC experiments were performed. In freshly prepared hIAPP(20–29) sample (HFIP- and sonication-treated), a relatively small trimer peak (20.1 min) followed by a large monomer peak (21.2 min) was observed, whereas in pIAPP(20–29), a dimer peak (20.5 min) was identified as the major peak, with no obvious monomer or trimer peak being identified. It is of interest to note that 20R-hIAPP(20–29) showed an intermediate SEC profile between that of pIAPP(20–29) and hIAPP(20–29), with a major monomeric peak (21.2 min) being found to coexist with a small dimer shoulder (~20.6 min) (Fig. 4). However, in all three decapeptide fragments, a similar hexamer peak (18.9 min) was found (Fig. 4).

Further SEC-monitored kinetics studies indicated markedly different oligomerization profiles during fibrillization of both hIAPP(20–29) and pIAPP(20–29). In hIAPP(20–29), a gradually diminishing trimer peak coupled with an ascending hexamer peak was observed as the incubation time increased (Supplementary Fig. S5). On the other hand, in pIAPP(20–29) samples, the dimer peak remain unchanged during the incubation, which is consistent with our ThT observation (Supplementary Fig. S5).

3.5. Cell viability assays

The aggregation of hIAPP(1–37) and its fragments, including hIAPP(17–29) and hIAPP(20–29), has been reported to exhibit cytotoxicity [4,18,20]. MTT assay was used to investigate the cytotoxicity of IAPP fragment variants in INS-1 cells. In our study, the hIAPP(1–37) at 20 μM exhibited a 75% toxic effect. At a concentration of 200 μM, hIAPP(20–29) and hIAPP(17–29) exhibited toxic effects of 40% and 31%, respectively, the highest in both the decapeptide and tridecapeptide sample groups, whereas pIAPP(20–29) and pIAPP(17–29) only showed 16% and 21% cytotoxicity, respectively, giving the lowest cytotoxicity in both groups. Moreover, our results clearly suggested that the 20R substitution significantly reduced the toxicity of hIAPP fragments (17% vs. 40% for decapeptide, and 21% vs. 31% for tridecapeptide, Fig. 5). Varied degrees of cytotoxicity were also observed for the rest of the decapeptide and tridecapeptide variants (Supplementary Figs. S8 and S9). However, at 100 μM concentration, hIAPP fragments (hIAPP(17–29) and hIAPP(20–29)) were only slightly more toxic compared with pIAPP fragments (pIAPP(17–29) and pIAPP(20–29)) (Fig. 5 and Supplementary Fig. S8).

4. Discussion

Not all species develop islet amyloid in vivo [3,21,22]. Rat IAPP (rIAPP) is well-known for amyloid-resistance. It has been suggested that hIAPP(17–29), especially the 20–29 region, is the major fragment for the formation of toxic hIAPP amyloid deposits [3]. The sequences of rIAPP and hIAPP differ at six of 37 positions, all

Table 1
Amyloidogenic properties of peptide fragments.[a]

	Peptides	Substitution(s)	Fibril formation[b]			
			Prediction[c]	Lag time (min)	t_{50} (min)	Amyloidogenic[d]
Human	1–37[e]	–	−5.6	0 ± 0	27.2 ± 20.7	+++
	17–29	–	1.0	39.1 ± 10.0	80.7 ± 28.5	+++
	17–29	D17	−14.8	66.9 ± 12.9	83.0 ± 4.4	++
	17–29	D17, R18	−16.1	64.7 ± 17.5	69.4 ± 15.2	++
	17–29	D17, R18, R20	−24.8	283.8 ± 88.2	370.7 ± 119.2	+
	17–29	D17, R20	−23.5	329.2 ± 30.7	406.7 ± 29.6	+
	17–29	R20	−7.7	241.5 ± 114.0	335.0 ± 179.6	+++
	20–29	–	10.8	39.6 ± 15.7	64.3 ± 15.6	+++
	20–29	R20	5.2	401.4 ± 116.4	429.3 ± 117.2	++
	20–29	G20	9.4	12.5 ± 3.6	25.5 ± 12.6	+++
	20–29	K20	7.0	288.2 ± 24.7	390.7 ± 80.1	+
	20–29	F27	14.6	252.9	280.0	+
	20–29	T25	6.4	73.6 ± 43.5	121.4 ± 66.9	+++
	20–29	L23	9.6	73.6 ± 43.5	121.4 ± 66.9	+++
Porcine	17–29	–	−25.9	1440+	–	–
	17–29	V17	−10.1	500+	–	–
	17–29	H18	−24.7	500+	–	–
	17–29	V17,H18	−8.8	500+	–	–
	17–29	V17,H18,S20	−0.1	500+	–	–
	17–29	V17,S20	−1.4	500+	–	–
	17–29	H18,S20	−15.9	500+	–	–
	17–29	S20	−17.2	500+	–	–
	20–29	–	3.0	2400+	–	–
	20–29	S20	8.6	500+	–	–
Cat	20–29	–	6.1	184.2 ± 43.7	245.3 ± 51.8	+
	17–29	–	−2.3	104.0 ± 81.6	147.0 ± 90.6	++
	17–29	H18	−1	48.9 ± 14.0	122.8 ± 57.8	++
Seeding	hIAPP(20–29) seeded with hIAPP(20–29)			15.7 ± 5.3	50.3 ± 22.1	+++
	20R-hIAPP(20–29) seeded with 20R-hIAPP(20–29)			184.6 ± 32.2	226.0 ± 41.3	++
	20R-hIAPP(20–29) seeded with hIAPP(20–29)			181.5 ± 90.1	240.0 ± 95.4	+++
	pIAPP(20–29) seeded with hIAPP(20–29)			500+	–	–
	hIAPP(20–29) seeded with 20R-hIAPP(20–29)			65.6 ± 3.9	89.3 ± 1.3	+++

[a] All assays were repeated for at least three times except 27F-hIAPP(20–29), which was performed for once due to limited sample supply.
[b] All samples were studied at 100 μM concentration except hIAPP(1–37), which was studied at 20 μM.
[c] Prediction values were calculated with the program Aggrescan [13], peptides are less prone to form amyloid with lower values [13].
[d] Semi-quantitative analysis of ThT-fluorescence based amyloid formation: "+++" designates samples with fluorescence intensity change greater than 40 arbitrary units, "++" for values between 10 and 40 arbitrary units, "+" for values between 1 and 10 arbitrary units, and "−" for values less than 0.1 arbitrary units.
[e] hIAPP(1–37) shows zero lag time in our assays, which may due to the fast stirring and high salt concentration used in the assay.

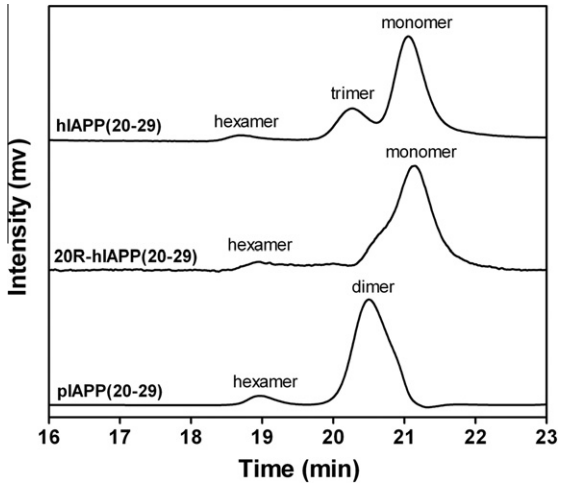

Fig. 4. Size-exclusion gel filtration profiles of different IAPP(20–29) fragments.

located in the region within residues 17–29 (Fig. 1). Extensive studies have been carried out to investigate how these variations affect amyloidogenicity, and two proline residues (25P and 28P) have been suggested to play more critical roles than 18H, 23L, 26V and 29P in resisting amyloid-formation [3]. Surprisingly, it has been reported that a single arginine to histidine substitution at position 18 abolishes the amyloid-resistant property of rIAPP and renders this variant capable of forming fibrils [23]. Full-length pIAPP has recently been reported to be refractory to amyloid formation [4]. Interestingly, the region of residues 17–29 also hosts seven out of 10 variation sites (Fig. 1), suggesting the important role this region played in amyloidogenic determination. Here, we demonstrated for the first time that both pIAPP(17–29) and pIAPP(20–29) were resistant to form amyloid in vitro under physiological conditions and that these fragments were also significantly less cytotoxic compared with the corresponding human fragments. Of all single-substitutions tested, we found each porcine substitution caused certain degrees of delayed lag time, but none of them could abolish the fibrillation of hIAPP(17–29) or hIAPP(20–29). On the other hand, none of the human substitutions (single or combined) could cause pIAPP(20–29) or pIAPP(17–29) fragments to gain amyloidogenic properties, which is different from the previous report that single human substitutions like R18H, L23F and V26I could cause amyloid-formation in rIAPP [23]. Thus, we conclude that the amyloidogenic properties of pIAPP and hIAPP are due to the combined effects of multiple site substitutions.

Of special interest, we identified position 20 as a critical site in determining the amyloidogenicity. Position 20 has been reported to relate to an inheritable T2DM which is mostly identified in Asia and Africa [24–26]. It has been reported that a 20G mutation could

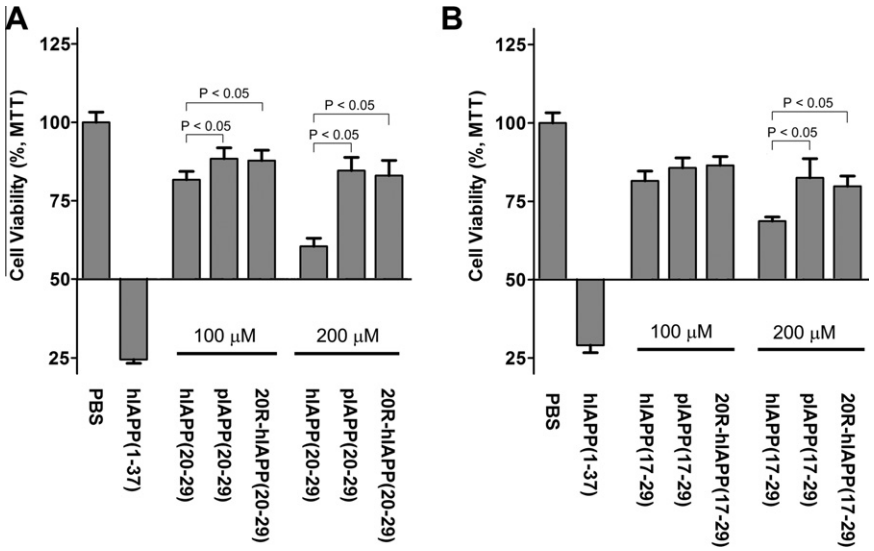

Fig. 5. Cell viability determined by MTT assay. (A) Cytotoxicity of IAPP(20–29) fragments at concentrations of 100 μM and 200 μM. (B) Cytotoxicity of IAPP(17–29) fragments at concentrations of 100 μM and 200 μM. Peptides are as labeled. 20 μM hIAPP(1–37) was used as the positive control.

cause accelerated fibrillation of hIAPP [27,28], which is in good accord with our observations on 20G-hIAPP(20–29). Moreover, the facts that the 20R substitution caused the most prolonged lag time and greatly attenuated the cytotoxicity of hIAPP further suggest the importance of this site in determining the propensity of amyloidogenic and cytotoxicity. Furthermore, the significantly prolonged lag time of the control analog 20K-hIAPP(20–29) suggested that the positive charge and/or the bulky side-chain may place a barrier to the assembly of amyloid aggregates.

The oligomerization states of IAPP and related fragments have been studied mostly by molecular dynamics simulation and experimental evidence is still necessary [29–31]. The present gel filtration study revealed different oligomerization properties of fragments of hIAPP and pIAPP. In hIAPP(20–29), monomeric, trimeric and a small amount of hexameric forms were observed, and the kinetic assay suggested that as the fibrillation went on, the trimer population starts diminishing while the population of higher molecular weight oligomers (mostly hexamers) gradually increases (Supplementary Fig. S5). However, in the corresponding pIAPP fragments, a major dimer peak was found, which remain essentially unchanged during incubation (Fig. 4 and Supplementary Fig. S5), suggesting that this dimer may be quite stable in solution. Similarly, the observation that the oligomerization profile of 20R-hIAPP(20–29) lies between that of pIAPP(20–29) and hIAPP(20–29) suggested that the 20R substitution may disrupt the trimer assembly and favor the formation of both dimers and monomers. To our knowledge, this is the first report that proved the existence of hIAPP(20–29) trimers, although its existence has been predicted by in silico molecular dynamics simulations [30]. On the other hand, we were unable to identify a hIAPP(20–29) dimer as another molecular dynamics simulation study suggested [31]. The existence of pIAPP(20–29) dimers has not been reported. We speculate that the intermolecular forces that stabilize this dimer may be critical to the prolonged fibrillation lag times. It has been reported by Raleigh et al. that rIAPP exists in solution as a monomer [32], indicating that pIAPP(20–29) may gain its fibril-resisting capacity with a novel dimer-forming mechanism.

Although the exact spatial structure of hIAPP amyloid remains unknown, accumulating structural evidence suggests that hIAPP molecule may adapt a β-hairpin like structure in the protofibril as well as in mature "cross-β" amyloid fibrils, in which residue 20 is located in the middle of the β-turn [33]. In support of this idea, a recent study on hIAPP and rIAPP demonstrated that the aggregation-prone hIAPP forms intramolecular β-turn more readily than rIAPP [34]. Techniques including X-ray fiber diffraction, electron diffraction, cryo-EM, FTIR, solid-state NMR and molecular dynamics simulations have been intensively applied to determine the fibril structure of hIAPP fragments, for example hIAPP(20–29), hIAPP(21–27), hIAPP(28–33) [20,35–37], with all results suggesting that the amyloidogenic region 20–29 adopts a steric zipper structure and further forms the cross-β spine of hIAPP amyloid [38]. Based on these observations, we proposed a possible amyloid-resistance mechanism for pIAPP in which the formation of stable dimers prevents peptides from further assembling into the β-turn structure and also the formation of the following nucleus and ordered mature fibrils (Fig. 6).

Peptide fragment-based hIAPP inhibitors have been previously constructed with good inhibitory effects [6,39,40]. It will also be of future interest to study the possibility of developing pIAPP

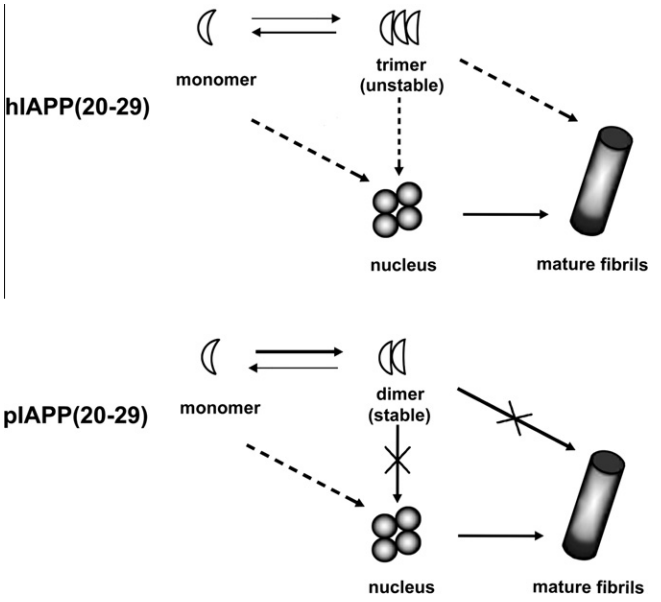

Fig. 6. Postulated role of oligomerization in the formation of mature IAPP(20–29) amyloid.

sequences based on hIAPP amyloid inhibitors and explore their potential therapeutic usages in T2DM.

Acknowledgments

This work was supported by the Natural Science Foundation of China (Nos. 30801445, 30970607 and 30870949), the National Basic Research Program of China (2009CB918304), Program for New Century Excellent Talents in University (NECT-10-0623), the Key Project of Chinese Ministry of Education (No. 109103), the Fundamental Research Funds for the Central Universities and the Important National Science and Technology Specific Projects (2009ZX09301-014). The authors wish to thank Dr. Mitchell Sullivan (University of Queensland) for proofreading the manuscript. The authors wish to express their appreciation to reviewers from the *FEBS Letters* journal for their insightful comments and suggestions.

Appendix A. Supplementary data

Supplementary data associated with this article can be found, in the online version, at doi:10.1016/j.febslet.2010.11.050.

References

[1] Clark, A., Charge, S.B., Badman, M.K., MacArthur, D.A. and de Koning, E.J. (1996) Islet amyloid polypeptide: actions and role in the pathogenesis of diabetes. Biochem. Soc. Trans. 24, 594–599.
[2] Johnson, K.H., O'Brien, T.D., Betsholtz, C. and Westermark, P. (1989) Islet amyloid, islet-amyloid polypeptide, and diabetes mellitus. New Engl. J. Med. 321, 513–518.
[3] Westermark, P., Engstrom, U., Johnson, K.H., Westermark, G.T. and Betsholtz, C. (1990) Islet amyloid polypeptide: pinpointing amino acid residues linked to amyloid fibril formation. Proc. Natl. Acad. Sci. USA 87, 5036–5040.
[4] Potter, K.J. et al. (2010) Islet amyloid deposition limits the viability of human islet grafts but not porcine islet grafts. Proc. Natl. Acad. Sci. USA 107, 4305–4310.
[5] Johnson, K.H., O'Brien, T.D., Betsholtz, C. and Westermark, P. (1992) Islet amyloid polypeptide: mechanisms of amyloidogenesis in the pancreatic islets and potential roles in diabetes mellitus. Lab. Invest. 66, 522–535.
[6] Scrocchi, L.A., Chen, Y., Waschuk, S., Wang, F., Cheung, S., Darabie, A.A., McLaurin, J. and Fraser, P.E. (2002) Design of peptide-based inhibitors of human islet amyloid polypeptide fibrillogenesis. J. Mol. Biol. 318, 697–706.
[7] Abedini, A. and Raleigh, D.P. (2006) Destabilization of human IAPP amyloid fibrils by proline mutations outside of the putative amyloidogenic domain: is there a critical amyloidogenic domain in human IAPP? J. Mol. Biol. 355, 274–281.
[8] Huang, K. et al. (2007) The A-chain of insulin contacts the insert domain of the insulin receptor. Photo-cross-linking and mutagenesis of a diabetes-related crevice. J. Biol. Chem. 282, 35337–35349.
[9] Huang, K., Maiti, N.C., Phillips, N.B., Carey, P.R. and Weiss, M.A. (2006) Structure-specific effects of protein topology on cross-beta assembly: studies of insulin fibrillation. Biochemistry 45, 10278–10293.
[10] Sreerama, N. and Woody, R.W. (2000) Estimation of protein secondary structure from circular dichroism spectra: comparison of CONTIN, SELCON, and CDSSTR methods with an expanded reference set. Anal. Biochem. 287, 252–260.
[11] Huang, K., Dong, J., Phillips, N.B., Carey, P.R. and Weiss, M.A. (2005) Proinsulin is refractory to protein fibrillation: topological protection of a precursor protein from cross-beta assembly. J. Biol. Chem. 280, 42345–42355.
[12] Konno, T., Oiki, S. and Morii, T. (2007) Synergistic action of polyanionic and non-polar cofactors in fibrillation of human islet amyloid polypeptide. FEBS Lett. 581, 1635–1638.
[13] Cabaleiro-Lago, C., Lynch, I., Dawson, K.A. and Linse, S. (2010) Inhibition of IAPP and IAPP(20–29) fibrillation by polymeric nanoparticles. Langmuir 26, 3453–3461.
[14] Conchillo-Sole, O., de Groot, N.S., Aviles, F.X., Vendrell, J., Daura, X. and Ventura, S. (2007) AGGRESCAN: a server for the prediction and evaluation of "hot spots" of aggregation in polypeptides. BMC Bioinform. 8, 65.
[15] Hettmansperger, T.P. and McKean, J.W. (1998) Robust Nonparametric Statistical Methods, John Wiley & Sons, Inc., NJ.
[16] Kayed, R., Bernhagen, J., Greenfield, N., Sweimeh, K., Brunner, H., Voelter, W. and Kapurniotu, A. (1999) Conformational transitions of islet amyloid polypeptide (IAPP) in amyloid formation in vitro. J. Mol. Biol. 287, 781–796.
[17] Abedini, A. and Raleigh, D.P. (2005) The role of His-18 in amyloid formation by human islet amyloid polypeptide. Biochemistry 44, 16284–16291.
[18] Pappalardo, G., Milardi, D., Magri, A., Attanasio, F., Impellizzeri, G., La Rosa, C., Grasso, D. and Rizzarelli, E. (2007) Environmental factors differently affect human and rat IAPP: conformational preferences and membrane interactions of IAPP17–29 peptide derivatives. Chemistry 13, 10204–10215.
[19] Madine, J., Jack, E., Stockley, P.G., Radford, S.E., Serpell, L.C. and Middleton, D.A. (2008) Structural insights into the polymorphism of amyloid-like fibrils formed by region 20–29 of amylin revealed by solid-state NMR and X-ray fiber diffraction. J. Am. Chem. Soc. 130, 14990–15001.
[20] Tenidis, K. et al. (2000) Identification of a penta- and hexapeptide of islet amyloid polypeptide (IAPP) with amyloidogenic and cytotoxic properties. J. Mol. Biol. 295, 1055–1071.
[21] Jordan, K., Murtaugh, M.P., O'Brien, T.D., Westermark, P., Betsholtz, C. and Johnson, K.H. (1990) Canine IAPP cDNA sequence provides important clues regarding diabetogenesis and amyloidogenesis in type 2 diabetes. Biochem. Biophys. Res. Commun. 169, 502–508.
[22] O'Brien, T.D., Westermark, P. and Johnson, K.H. (1990) Islet amyloid polypeptide (IAPP) does not inhibit glucose-stimulated insulin secretion from isolated perfused rat pancreas. Biochem. Biophys. Res. Commun. 170, 1223–1228.
[23] Green, J., Goldsbury, C., Mini, T., Sunderji, S., Frey, P., Kistler, J., Cooper, G. and Aebi, U. (2003) Full-length rat amylin forms fibrils following substitution of single residues from human amylin. J. Mol. Biol. 326, 1147–1156.
[24] Sakagashira, S., Sanke, T., Hanabusa, T., Shimomura, H., Ohagi, S., Kumagaye, K.Y., Nakajima, K. and Nanjo, K. (1996) Missense mutation of amylin gene (S20G) in Japanese NIDDM patients. Diabetes 45, 1279–1281.
[25] Lee, S.C., Hashim, Y., Li, J.K., Ko, G.T., Critchley, J.A., Cockram, C.S. and Chan, J.C. (2001) The islet amyloid polypeptide (amylin) gene S20G mutation in Chinese subjects: evidence for associations with type 2 diabetes and cholesterol levels. Clin. Endocrinol. (Oxf.) 54, 541–546.
[26] Yamada, K., Yuan, X., Ishiyama, S. and Nonaka, K. (1998) Glucose tolerance in Japanese subjects with S20G mutation of the amylin gene. Diabetologia 41, 125.
[27] Sakagashira, S., Hiddinga, H.J., Tateishi, K., Sanke, T., Hanabusa, T., Nanjo, K. and Eberhardt, N.L. (2000) S20G mutant amylin exhibits increased in vitro amyloidogenicity and increased intracellular cytotoxicity compared to wild-type amylin. Am. J. Pathol. 157, 2101–2109.
[28] Ma, Z. et al. (2001) Enhanced in vitro production of amyloid-like fibrils from mutant (S20G) islet amyloid polypeptide. Amyloid 8, 242–249.
[29] Zanuy, D. and Nussinov, R. (2003) The sequence dependence of fiber organization. A comparative molecular dynamics study of the islet amyloid polypeptide segments 22–27 and 22–29. J. Mol. Biol. 329, 565–584.
[30] Mo, Y., Lu, Y., Wei, G. and Derreumaux, P. (2009) Structural diversity of the soluble trimers of the human amylin(20–29) peptide revealed by molecular dynamics simulations. J. Chem. Phys. 130, 125101.
[31] Rivera, E., Straub, J. and Thirumalai, D. (2009) Sequence and crowding effects in the aggregation of a 10-residue fragment derived from islet amyloid polypeptide. Biophys. J. 96, 4552–4560.
[32] Cao, P., Meng, F., Abedini, A. and Raleigh, D.P. (2010) The ability of rodent islet amyloid polypeptide to inhibit amyloid formation by human islet amyloid polypeptide has important implications for the mechanism of amyloid formation and the design of inhibitors. Biochemistry 49, 872–881.
[33] Luca, S., Yau, W.M., Leapman, R. and Tycko, R. (2007) Peptide conformation and supramolecular organization in amylin fibrils: constraints from solid-state NMR. Biochemistry 46, 13505–13522.
[34] Dupuis, N.F., Wu, C., Shea, J.E. and Bowers, M.T. (2009) Human islet amyloid polypeptide monomers form ordered beta-hairpins: a possible direct amyloidogenic precursor. J. Am. Chem. Soc. 131, 18283–18292.
[35] Elgersma, R.C., Mulder, G.E., Kruijtzer, J.A., Posthuma, G., Rijkers, D.T. and Liskamp, R.M. (2007) Transformation of the amyloidogenic peptide amylin(20–29) into its corresponding peptoid and retropeptoid: access to both an amyloid inhibitor and template for self-assembled supramolecular tapes. Bioorg. Med. Chem. Lett. 17, 1837–1842.
[36] Nielsen, J.T. et al. (2009) Unique identification of supramolecular structures in amyloid fibrils by solid-state NMR spectroscopy. Angew. Chem., Int. Ed. Engl. 48, 2118–2121.
[37] Wiltzius, J.J., Sievers, S.A., Sawaya, M.R., Cascio, D., Popov, D., Riekel, C. and Eisenberg, D. (2008) Atomic structure of the cross-beta spine of islet amyloid polypeptide (amylin). Protein Sci. 17, 1467–1474.
[38] Sawaya, M.R. et al. (2007) Atomic structures of amyloid cross-beta spines reveal varied steric zippers. Nature 447, 453–457.
[39] Potter, K.J. et al. (2009) Amyloid inhibitors enhance survival of cultured human islets. Biochim. Biophys. Acta 1790, 566–574.
[40] Moriarty, D.F. and Raleigh, D.P. (1999) Effects of sequential proline substitutions on amyloid formation by human amylin20–29. Biochemistry 38, 1811–1818.